

COMPUTATIONAL STUDY OF THE AERODYNAMIC CHARACTERISTICS OF AXI-SYMMETRIC BODIES IN TRANSONIC FLOW¹

Eddy Priyono² and Harijono Djojodihardjo³

Department of Aeronautics and Astronautics, Bandung Institute of Technology

Jl. Ganesha 10 Bandung, Indonesia

e-mail : hardjojo@cbn.net.id

Keywords: Aerodynamics, Computational Fluid Dynamics, Optimization, Slenderbody, Transonic Flow

ABSTRACT

Extensive work on slender axi-symmetric bodies in transonic flow has been carried out and well documented in the 1970's. With the progress of CFD that has taken place in the following decades, codes are available to look into the detailed characteristics of the shock-boundary layer interaction and the resulting wave drag, in particular due to the geometry of the afterbody. However, to the authors' knowledge, the optimum drag of axi-symmetric bodies need further elaboration. Therefore it is the objective of present work look carefully into the drag mechanism due to geometry of the afterbody, in particular and more significantly, to find a way to optimize the total drag.

Three steps of approaches are be followed. The first approach will review selected analytical methods in the calculation of the aerodynamic characteristics of slender-axisymmetric bodies in transonic flow, in particular the classical approach of Ashley and Landahl. A more recent work of Biblarz introduced variable transformation that allows analytical solution of the linearized gas dynamic transonic equation, that yields a family of slender axi-symmetric bodies as one of the closed form solutions of the equation. These aerodynamic bodies can be used as initial references in an optimization approach. The second parts deals with the systematic determination of an optimum slender axi-symmetric body configuration based on aerodynamic characteristics criteria. The simplest one is the minimization of the pressure (wave) drag. Sequential Quadratic Programming using BFGS technique as well as Modified Feasible Direction (MFD) method with constraint optimization can be applied. The solution will be an intermediate one that has to be checked using more accurate solutions of the Euler or Navier Stokes equation. To this end numerical approaches are carried out, which can also be utilized to study slender bodies with various after body configurations and to arrive at the optimum drag configuration. Two numerical approaches can be followed; using the well established computational

fluid dynamic method in solving the Euler and the Navier-Stokes equation around an axi-symmetric body in transonic flow.

1. Introduction

The drag minimization of slender axisymmetric body, particularly in the transonic flow regime, has received much interest. Such situation is encountered, for example, in the design for minimum drag of projectile geometries. Noting the transonic nature of the significant part of the prevailing flow field, a computational study is performed on the aerodynamic characteristics a slender axi-symmetric body in transonic flow. The presence of shock wave should be minimized; the geometry of the afterbody, which has been the subject of many previous investigations, should be carefully studied and optimized. In addition to the presence of the shock wave, the base pressure characteristics contribute significantly to the drag.

Three steps of approaches then can be followed; each is considered to have significant merit and contribution to the effort. The first approach will review selected analytical methods in the calculation of the aerodynamic characteristics of slender-axisymmetric bodies in transonic flow, in particular the classical approach of Ashley and Landahl [1]. This method is analytical, elegant and reveals the generic contributions of geometrical elements to the drag, and will be useful in estimating the characteristics of several slender axi-symmetric body configurations, such as those described by Krasnov[2], and Cuong and Norstrud[3], or other generic configurations. A more recent work (Biblarz[4], Biblarz and Priyono[5]) is of interest and introduced variable transformation that allows analytical solution of the linearized gas dynamic transonic equation. This method yields a family of slender axi-symmetric bodies as one of the closed form solutions of the equation. These aerodynamic bodies can be used as initial references in an

¹ For presentation at the 23rd ICAS Congress, Toronto, Canada, 8-13 September 2002.

² Faculty Member, Nurtanio Institute of Technology and PhD Student, Institute of Technology Bandung

³ Professor, Department of Aeronautics and Astronautics, Institute of Technology Bandung

optimization approach to obtain ones with certain desired aerodynamic characteristics, which is the main objective of the study.

The second part deals with the systematic determination of an optimum slender axi-symmetric body configuration based on aerodynamic characteristics criteria. The simplest one is the minimization of the pressure (wave) drag. To this end, the minimization problem and procedure (Vanderplaats [6][7]) will be formulated and resort will be made to commercially available solvers, in particular MATLAB®, in reaching the desired solution.

Since in reaching the desired configuration first order analytical approaches have been utilized for efficiency, there is a need to evaluate as well as to obtain more accurate and detailed aerodynamic characteristics of the selected geometries.

To this end numerical approaches are carried out to study slender bodies with various after body configurations and to arrive at the optimum drag configuration. This can be carried out by inspection or by incorporating the numerical evaluation in the optimization procedure, such as by following the philosophy described by Vanderplaats[7]. In the study, two numerical approaches are carried out; the first use the well established computational fluid dynamic method in solving the Euler equation around a slender axi-symmetric body in transonic flow, and the second uses the Navier-Stokes flow solvers, both the commercially available ones,

The computational results have been validated by comparing the results for known geometric configurations and flow conditions with standard ones. The characteristics of the flow field can be utilized in working for the desired optimum characteristics, in particular in obtaining geometries with minimum drag.

In looking for the candidates of geometries with minimum drag, three projectiles configurations that are considered convenient are utilized, each characterized by flat, conical and rounded afterbody. Analysis are carried out for projectiles moving without spin. For the numerical computation of the flow characteristics (such as Mach contour, pressure coefficient (Cp), and Drag Coefficient (Cd)), commercially available flow solvers are utilized; these are Multi Grid Aerodynamics (MGAERO) and RAMPANT Flow Solvers, for solving the Euler and Navier-Stokes Equations, respectively.

2. Parametric Study of the afterbody geometry of Slender Axi-Symmetrical Body moving in Transonic Flow using classical approach as a baseline in optimization scheme

For slender bodies moving in transonic flow using small perturbation approach, one can start with the following gas dynamic equation in cylindrical coordinate system:

$$(1-M_\infty^2) \frac{\partial^2 \phi}{\partial x^2} + \frac{\partial^2 \phi}{\partial r^2} + \frac{1}{r} \frac{\partial \phi}{\partial r} + \frac{1}{r^2} \frac{\partial^2 \phi}{\partial \theta^2} = \frac{M_\infty^2 (\gamma+1)}{U} \frac{\partial \phi}{\partial x} \frac{\partial^2 \phi}{\partial x^2} \quad (1)$$

Where x is in the axial direction.

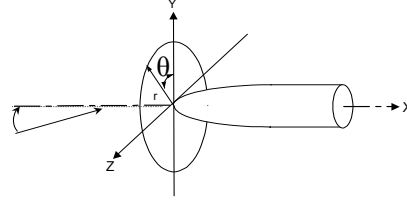


Fig. 1 Polar Coordinate system

Next, for axi-symmetrical slender body moving in transonic potential flow, and following *Small Perturbation Theory*, higher order terms are ignored, equation (1) can be written in the following form:

$$\frac{1}{r} \frac{\partial}{\partial r} (r \phi_r) + (1-M_\infty^2) \phi_{xx} = \phi_x \phi_{xx} \quad (2)$$

Following Ashley and Landahl [1] the drag of the axi-symmetrical slender body moving in transonic potential flow, can be written as:

$$\frac{D}{\rho U_\infty^2} = -\frac{1}{2\pi} \int_0^l S''(x) dx \int_0^x S'''(x_1) \ln(x-x_1) dx_1 \quad (3)$$

if the afterbody ends through a smooth curve that ends at the axis (without a flat base), where S is the area of the cross section of the slender body and the prime and double prime indicates its first and second derivatives with respect to the x axis, respectively. This expression is amenable to parametric study of the slender axi-symmetric body with various afterbody geometries, at least for the preliminary steps.

Some families of generating curves for the afterbody geometries will be studied, the simplest one being a polynomial of the form:

$$R(x) = Y_1 (1-x^{n1}) + Y_2 (1-x^{n2}) + Y_3 (1-x^{n3}) + Y_4 (1-x^{n4}) \quad (4)$$

where R is the radius of the slender body as a function of x and $\mathbf{Y} = \{ Y_1, Y_2, Y_3, Y_4 \}^T$ could be used as the solution vector representing the afterbody geometry and in minimizing the drag

as represented by formula (3) as the objective function in the minimization process. More generally, higher order polynomials can be utilized, but representation (4) is considered to be instructive in developing the method. The choice of the powers n_1, n_2, n_3 and n_4 is at our disposal, and can be decided by inspecting the generic geometrical shape given by each, such as by $(1-x^4)$. For convenience, in the computational procedure non-dimensional variables have been used. For this purpose, for example, in the study, it is required that

$$\mathbf{Y}_1 + \mathbf{Y}_2 + \mathbf{Y}_3 + \mathbf{Y}_4 = 1 \quad (5)$$

Other geometries, such as the tanh function as suggested by Nghiem and Norstrud[3], as well as geometries formulated by Biblarz [4][5], Priyono [8] and Priyono and Djodihardjo[9], can be approximated by using representation (4). Certainly other series approximations can also be utilized, which could be chosen from their closeness to the anticipated or desired geometry, and ease for analysis. The geometry resulted from Biblarz analysis (for convenience referred to as Biblarz curve) can also be approximated by the polynomial (5).

These geometries are utilized in studying the parametric behavior of the flow characteristics, and serve as references in numerical solutions obtained by solving more exact differential equations, as given by the Euler equation for the inviscid approximation and the Navier-Stokes equation for the viscous case. The flow characteristics, in particular the pressure distribution along the surface of the body, can readily be calculated [5][8], which then can be used in studying the drag of the body. The characteristics of the flow field can be utilized in working for desired optimum characteristics, in particular in obtaining geometries with minimum drag.

Another search for the candidate geometries with minimum drag is carried out by studying the aerodynamic characteristics of three projectile configurations that are considered convenient; these are slender axisymmetrical bodies with flat, conical and rounded afterbody. All of our analyses are carried out for slender bodies moving without spin. For the numerical computation of the flow characteristics (such as Mach contour, pressure coefficient (C_p), and Drag Coefficient (C_d)), commercially available flow solvers are utilized; these are *Multi Grid Aerodynamics* (MGAERO) and *RAMPANT Flow Solvers*, for solving the Euler and Navier-Stokes Equations, respectively.

3. Geometrical Optimization Scheme

To obtain afterbody geometries with minimum aerodynamic drag, two approaches can be carried out.

The most straightforward one is by direct computation of a set of geometries selected from some physical or analytical configurations, while the second is a systematic one following a wellknown optimization scheme. The first approach is simple and straightforward, which can be carried out utilizing physical considerations and intuition, but will be time consuming and mathematically speaking, does not guarantee a globally optimum configuration. It can only serve as an illustration. The second approach follows some well known optimization scheme, such as by using Sequential Quadratic Programming or Modified Feasible Direction method [6][7]. These methods are considered to be effective and accurate in reaching a globally optimum configuration.

The Modified Feasible Direction method requires that an initial set of design variables, \mathbf{Y}^0 be specified. Beginning from this starting point, the design is updated iteratively. The most common form of this iterative procedure is given by :

$$\mathbf{Y}^q = \mathbf{Y}^{q-1} + \mathbf{a}^* \cdot \mathbf{S}^q \quad (6)$$

Where :

- q = iteration number
- \mathbf{S} = vector search direction in the design space
- \mathbf{a}^* = scalar quantity defining the distance that we wish to move in the direction \mathbf{S}

The iterative relationship given by Eqs.(6) is applied to the optimization process, where \mathbf{Y} is the solution vector indicative of the geometry of the slender axisymmetrical body.

Let the drag $D = F(\mathbf{Y})$ is the objective function and $\mathbf{g}(\mathbf{Y})$ is the constraint function vector.

Assume we begin at point \mathbf{Y}^0 and we wish to reduce the objective function by searching in direction \mathbf{S}^1 .

The choice of \mathbf{S} is somewhat arbitrary as long as a small move in this direction will reduce the objective function without violating any constraints. In this case, the \mathbf{S}^1 vector is approximately the negative of the gradient of the objective function, i.e. the direction of steepest descent[6] . It is now necessary to find the scalar \mathbf{a}^* in Eqs.(6) so that the objective function is minimized in this direction without violating any constraints. In essence, the optimization of $D = F(\mathbf{Y})$ subject to the constraint function vector $\mathbf{g}(\mathbf{Y})$ can be generally stated as :

$$\text{Minimize: } D = F(\mathbf{Y}) \quad (7)$$

Subject to :

$$\mathbf{g}(\mathbf{Y}) \leq 0, \mathbf{g}(\mathbf{Y}) = \{ \mathbf{g}_j(\mathbf{Y}) \}, \quad j = 1, m$$

$$\begin{aligned} \mathbf{h}(\mathbf{Y}) &= 0, \mathbf{h}(\mathbf{Y}) = \{ \mathbf{h}_k(\mathbf{Y}) \}, & k &= 1, l \\ \mathbf{Y}_i^l &\leq \mathbf{Y}_i \leq \mathbf{Y}_i^u, & i &= 1, n \end{aligned} \quad (8)$$

where :

$F(\mathbf{Y})$ = objective function

$\mathbf{g}(\mathbf{Y})$ = inequality constraints

$\mathbf{h}(\mathbf{Y})$ = equality constraints

\mathbf{Y}_i^l = lower bound of solution vector components

\mathbf{Y}_i^u = upper bound of solution vector components

By appropriate formulation of the problem, solution procedure can readily be followed by resorting to standard Quadratic Sequential Programming Technique of Modified of Feasible Directions that are available in commercial software, such as MATLAB®.

It is noteworthy that in many of these methods, the Gradient Vector $\nabla F(\mathbf{Y}^0)$ as well as the Hessian Matrix \mathbf{H} of the Second Derivatives of the Objective function have to be computed. vector which reduces the objective function is called usable direction.

In the modified feasible direction method, the usability requirement is stated as the dot product of $\nabla F(\mathbf{Y}^0)$ and S should be negative, i.e.

$$\nabla F(\mathbf{Y}^0) \cdot S \leq 0$$

A direction is called feasible if for some small move in that direction, the active constraint will not be violated, thus the dot product of $\nabla g_i(X^0)$ and S must be negative:

$$\nabla g(\mathbf{Y}^0) \leq 0$$

In the present study, the systematic optimization scheme is carried out by using simple geometries characterized by equation.(4) and approximate drag formula (3). Then the minimum drag configuration obtained by the geometry optimization procedure is checked for its plausibility using more accurate methods described below. If the geometry has not met the requirements based on other considerations, the optimization procedure described above can be repeated with additional modification to the geometrical expression. Alternatively, several families of geometries can be compared to reach at desired configuration.

4. Parametric Study of the Flow Characteristics Of Slender Axi-Symmetric Bodies In Transonic Flow for the inviscid and the viscous case.

4.1 Numerical approach by Numerical Solution of the Euler Equation (inviscid case)

The first numerical approach utilized for the parametric study of the influence of the afterbody geometry to the drag is the numerical computational procedure to solve the inviscid Euler Equation. The prevailing governing equations which involve the mass, momentum and energy conservation equations can be written in the

conservation form, in the Two-Dimensional Cartesian coordinates (to attack the problems at hand) as follows:

$$\frac{\partial Q}{\partial t} + \frac{\partial E}{\partial x} + \frac{\partial F}{\partial y} + \alpha H = 0 \quad (9)$$

where:

$\alpha = 0$ for planar 2D flow

$\alpha = 1$ for axisymmetrical 2D flow

and where:

$$Q = \begin{bmatrix} \rho \\ \rho u \\ \rho v \\ \rho e_t \end{bmatrix}; E = \begin{bmatrix} \rho u \\ \rho u^2 + p \\ \rho uv \\ (\rho e_t + p)u \end{bmatrix} \quad (10)$$

$$F = \begin{bmatrix} \rho v \\ \rho vu \\ \rho v^2 + p \\ (\rho e_t + p)v \end{bmatrix}; H = \frac{1}{y} \begin{bmatrix} \rho v \\ \rho vu \\ \rho v^2 \\ (\rho e_t + p)v \end{bmatrix}$$

$$e_t = \frac{a^2}{\gamma(\gamma-1)} + \frac{1}{2}(u^2 + v^2) \quad (11)$$

To facilitate numerical computation, the above equation is written in Finite difference formulation. The time derivative is approximated by a first order backward difference quotient and the remaining terms are evaluated at time level $n + 1$. Then equation (9) can be written in finite difference formulation as:

$$\frac{\bar{Q}^{n+1} - \bar{Q}^n}{\Delta \tau} + \left(\frac{\partial \bar{E}}{\partial \xi} \right)^{n+1} + \left(\frac{\partial \bar{F}}{\partial \eta} \right)^{n+1} + \alpha (\bar{H})^{n+1} = 0 \quad (12)$$

Equation (12) is non-linear. Further simplification is afforded by linearized approach, which then yields:

$$\begin{aligned}\bar{E}^{n+1} &= \bar{E}^n + \left(\frac{\partial \bar{E}}{\partial \bar{Q}}\right) \Delta \bar{Q} + O(\Delta \tau)^2 \\ \bar{F}^{n+1} &= \bar{F}^n + \left(\frac{\partial \bar{F}}{\partial \bar{Q}}\right) \Delta \bar{Q} + O(\Delta \tau)^2 \\ \bar{H}^{n+1} &= \bar{H}^n + \left(\frac{\partial \bar{H}}{\partial \bar{Q}}\right) \Delta \bar{Q} + O(\Delta \tau)^2\end{aligned}\quad (13)$$

where

$$\frac{\partial \bar{E}}{\partial \bar{Q}} = A \quad ; \quad \frac{\partial \bar{F}}{\partial \bar{Q}} = B \quad ; \quad \frac{\partial \bar{H}}{\partial \bar{Q}} = C \quad (14)$$

are Jacobian matrices.

The numerical computation then is carried out by solving the following equation in the computational grid.

$$\begin{aligned}\Delta \bar{Q} + \Delta \tau \left\{ \frac{\partial}{\partial \xi} [\bar{E}^n + A^n \bar{Q}] + \right. \\ \left. \frac{\partial}{\partial \eta} [\bar{F}^n + B^n \Delta \bar{Q}] + \alpha [\bar{H}^n + C^n \Delta \bar{Q}] \right\} = 0\end{aligned}\quad (15)$$

For this purpose, the commercially available flow solver *Multi Grid Aerodynamics* (MGAERO)[10] is utilized.

4.2 Parametric Study of the flow characteristics using MGAERO

The flow characteristics of projectiles with three different afterbody geometries are investigated, these are the flat edged, conical and rounded edge aft-bodies. The projectile, which is axi-symmetrical, does not rotate about its longitudinal axis, which is the axis of symmetry. In the analysis, Mach number, pressure coefficient (C_p), and drag coefficient (C_d) contours are obtained characterizing the resulting flow field.

4.2.1 Results

The calculation is carried out for three different values of free-stream Mach numbers, these are 0.8, 1.2 and 1.5; the angle of attack $\alpha = 0$.

4.2.2 Projectile with flat afterbody

The Mach contour and pressure distribution of the projectile with flat afterbody geometry under study are shown in Figs. 2a and 2b, respectively.

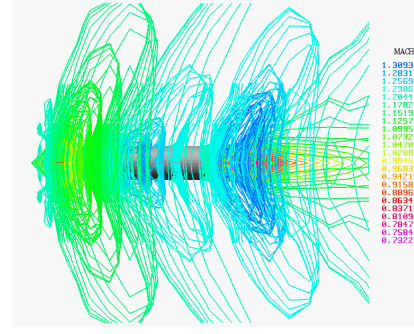


Fig. 2a Mach contour $M = 1.2$

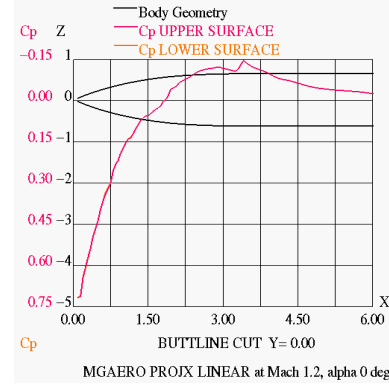


Fig. 2b Pressure Distribution C_p

In particular, for free stream Mach number $M = 1.2$, shocks occur at the bow and at the stern of the projectile. At $M = 0.8$ no shock wave occurs; at $M = 1.2$ and 1.5 , the presence of shockwaves is accompanied by the presence of mach lines that are inclined downstream. The pressure distribution indicates a maximum at the bow of the projectile, i.e the stagnation point, as expected, and decays towards downstream. At the stern, the pressure decreases sharply.

It should be noted, however, that at the afterbody region, the inviscid computational approach may not be valid without proper modeling of the flow. The results thus far obtained may be indicative of the real situation only at the upstream part, especially if there are shocks in the vicinity of the stern. It is with such notion in mind that the inviscid numerical approach is only utilized to obtain first hand solutions. It is with such notion in mind that further refinement of the results, if necessary, will be resorted to by the use of the direct numerical approach to the fully viscous flow.

4.2.3 Projectile with conical afterbody

Next, we will look into the second projectile with conical afterbody. The Mach contour and pressure distribution of the projectile with flat afterbody geometry under study are shown in Figs. 3a and 3b, respectively.

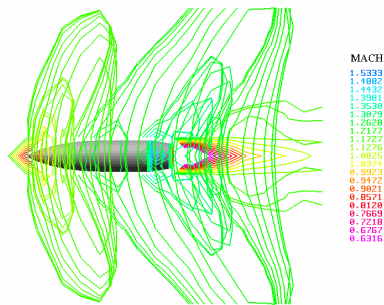


Fig. 3a Mach contour, M = 1.2

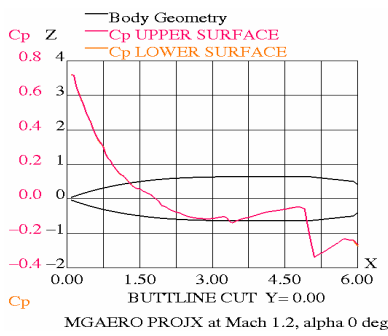


Fig 3b Pressure distribution

For this configuration, at free-stream Mach number $M = 0.8$, the local velocity is gradually accelerated downstream along the surface until near the stern, it reaches a value of $M = 1.4$. For $M = 1.2$ and 1.5 , shockwaves appear at the front and rear part. For $M = 0.8$, compared to the former geometry, the pressure drops near the beginning of the conical part of the afterbody due to expansion wave. For $M = 1.2$, expansion wave also occurs near the beginning of the conical part.

4.2.4 Projectile with rounded afterbody

Next, we will look into the second projectile with conical afterbody. The Mach contour and pressure distribution of the projectile with flat afterbody geometry under study are shown in Figs. 4a and 4b, respectively.

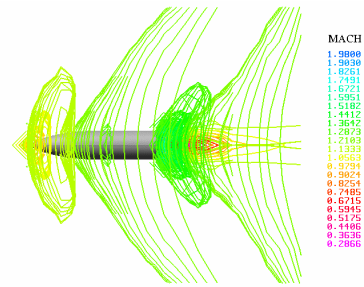


Fig. 4a Mach contour, M = 1.2

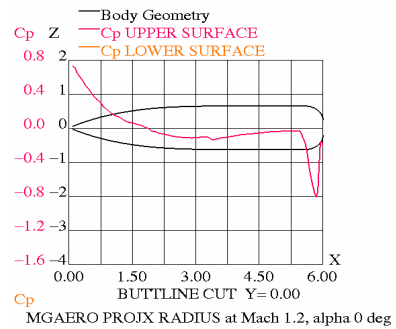


Fig. 4b Pressure Distribution Cp

For this configuration, at free-stream Mach number $M = 0.8$, the local velocity is also gradually accelerated downstream along the surface until near the stern, and it also reaches a value of $M = 1.4$ there. For $M = 1.2$ and 1.5 , shockwaves appear at the front and rear part. For $M = 0.8$ expansion wave occurs near the stern, as indicated also by a sharp pressure jump there. The pressure jump occurs at the rounded part of the stern. Comparing the pressure jump here for this geometry with that for the other geometries studied, the pressure jump here is relatively larger. The pressure jump here for $M = 0.8$ reaches -1.5 , while for the flat stern $= -0.16$ and for conical stern $= -0.60$.

4.2.5 Drag components

The following table summarizes the numerical results obtained for the drag components of the projectile for three different geometry studies. Among the three geometries, rounded stern seems to give rise to lower drag components, as indicated by Table 1.

Table 1 Drag components

No		Mach No.		
		0.8	1.2	1.5
I	Induced Drag (Cdi)			
	1. Flat	0.26145E-02	0.44473E-02	0.40776E-02
	2. Conical	0.10025E-02	0.29843E-02	0.28796E-02
	3. Rounded	0.52563E-03	0.24420E-02	0.26100E-02
II	Wave Drag			
	1. Flat	0.69328E-02	-0.42792E-01	0.28855E-02
	2. Conical	0.17599E-02	-0.38999E-01	0.10645E-01
	3. Rounded	0.12974E-02	-0.33929E-01	0.12927E-02

4.3 Numerical approach by Numerical Solution by Numerical Solution of the Navier Stokes (viscous case)

The numerical approach utilized for the parametric study of the influence of the afterbody geometry to the drag is the numerical computational procedure to solve the viscous Navier-Stokes Equation. For this purpose, commercially available *Rampant Flow Solver*[10] is utilized, since Rampant Flow Solver provides comprehensive modeling capabilities for a wide range of incompressible and compressible, laminar and turbulent fluid flow problems. Also, since Rampant has capabilities to solve flow model by using a reference of rotating frame, it can be utilized to analyze aerodynamic characteristic of axisymmetric slender body. One can take note that Rampant can solve the EULER equation as well NAVIER-STOKES equation for laminar viscous flow.

The prevailing governing equations which involve the mass, momentum and energy conservation equations can be written, in the conservation form and in the two-dimensional Cartesian coordinates (to attack the problems at hand), as follows:

$$\frac{\partial Q}{\partial t} + \frac{\partial E}{\partial x} + \frac{\partial F}{\partial y} + \alpha H = \frac{\partial E_v}{\partial x} + \frac{\partial F_v}{\partial y} + \alpha H_v \quad (20)$$

$$F_v = \begin{bmatrix} 0 \\ \tau_{xy} \\ \tau_{yy} \\ u\tau_{xy} + v\tau_{yy} - q_y \end{bmatrix} \quad (21)$$

$$H_v = \frac{1}{y} \begin{bmatrix} 0 \\ \tau_{xy} - \frac{2}{3} \frac{y}{Re_\infty} \frac{\partial}{\partial x} \left(\mu \frac{v}{y} \right) \\ \tau_{yy} - \tau_{\theta\theta} - \frac{2}{3} \frac{\mu}{Re_\infty} \left(\frac{v}{y} \right) - \frac{y}{Re_\infty} \frac{2}{3} \frac{\partial}{\partial y} \left(\mu \frac{v}{y} \right) \\ u\tau_{xy} + v\tau_{yy} - q_y - \frac{2}{3} \frac{\mu}{Re_\infty} \frac{v^2}{y} - \frac{y}{Re_\infty} \frac{\partial}{\partial y} \left(\frac{2}{3} \mu \frac{v^2}{y} \right) - \frac{y}{Re_\infty} \frac{\partial}{\partial x} \left(\frac{2}{3} \mu \frac{uv}{y} \right) \end{bmatrix}$$

a = 0 for planar 2D flow case and
a = 1 for axisymmetric 2D flow case

where :

$$Q = \begin{bmatrix} \rho \\ \rho u \\ \rho v \\ \rho e_t \end{bmatrix} ; E = \begin{bmatrix} \rho u \\ \rho u^2 + p \\ \rho uv \\ (\rho e_t + p)u \end{bmatrix}$$

$$F = \begin{bmatrix} \rho v \\ \rho vu \\ \rho v^2 + p \\ (\rho e_t + p)v \end{bmatrix} ; H = \frac{1}{y} \begin{bmatrix} \rho v \\ \rho vu \\ \rho v^2 \\ (\rho e_t + p)v \end{bmatrix}$$

$$E_v = \begin{bmatrix} 0 \\ \tau_{xyp} \\ \tau_{xy} \\ u\tau_{xyp} + v\tau_{xy} - q_x \end{bmatrix} \quad (22)$$

4.3.1 Results for axi-symmetric cases investigated using 3D Rampant Flow Solver.

The Mach contour and pressure distribution along the surface of the projectile investigated are shown for the projectile with flat base in Figs. 5a and 5b, respectively, with conical

afterbody in Figs. 6a and 6b, respectively, and with rounded afterbody in Figs. 7a and 7b, respectively.

Similar characteristics obtained by utilizing Navier-Stokes solver (RAMPANT) to those investigated using Euler solver (MGAERO) are indicated there. However, the flow situation near the base are better revealed. For the projectile with flat base, strong flow separation is clearly exhibited at the base. The stagnation pressure at the nose for $M = 1.2$ is stronger than that for $M = 0.8$ and $M = 1.5$, which may indicate the presence of stronger shocks (or shock-boundary layer interaction) along the surface of the projectile near sonic free stream speed.

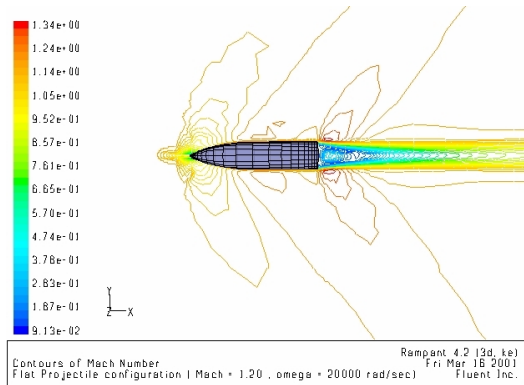


Fig 5a Mach contour M = 1.2 Flat base

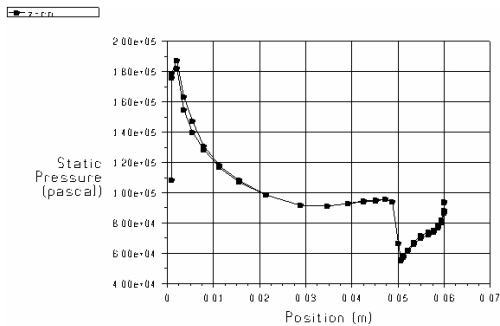


Fig 5b Cp Distribution M= 1.2 Flat base

Conical Afterbody

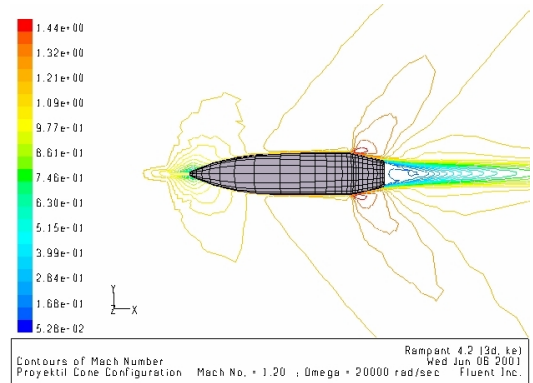


Fig 6a Mach contour

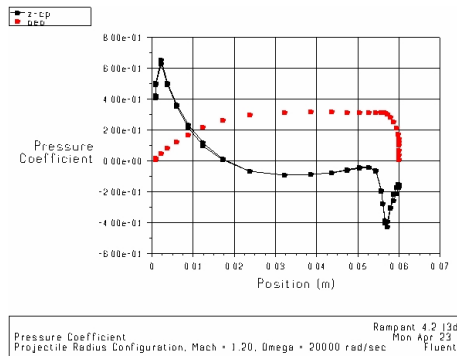


Fig 6b Cp Distribution

Rounded Afterbody

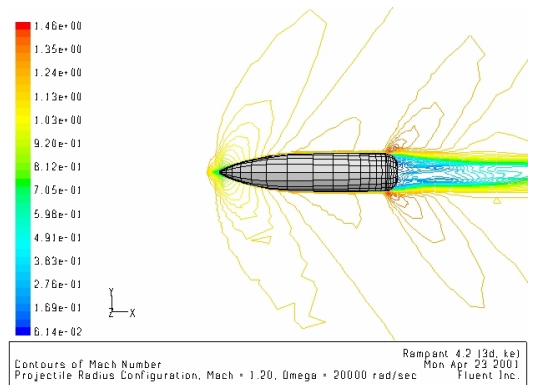


Fig 7a Mach contour

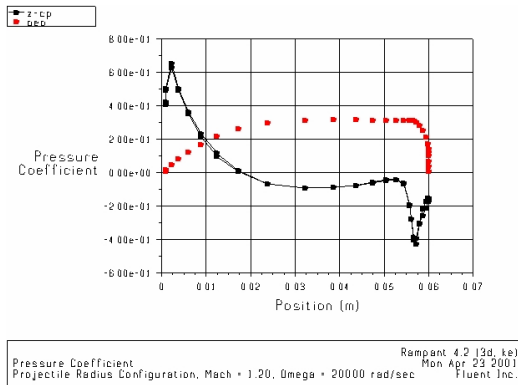


Fig 7 b Cp Distribution

Compared to the other two geometries, the rounded base configuration gives rise to stronger shock wave close to the base, close to the rounded surface.

4.3.2 Variation of Drag due to Mach number

The Navier Stokes flow solver has been applied for projectiles with the three different afterbody configurations for values of Mach number ranging from $M = 0.6$ to $M = 3.0$. The variation of drag (C_d) with respect to the Mach number is exhibited in Fig. 8. As already well known, the maximum drag occurs near the sonic free stream velocity. The search for the optimum geometry from the view point of drag can be focussed to this figure. Fig. 8 indicates that the projectile with rounded afterbody produces the best (minimum) drag characteristics among the three geometries investigated.

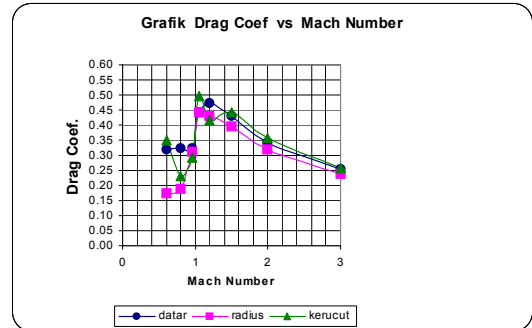


Fig 8 Cd vs M

5. Discussion of Drag Optimization Results

Drag optimization scheme as described in part 3 has given some feasible afterbody geometrical configurations, such as illustrated in Figure 8, found using optimization of curve (4) following problem formulation (8).

The geometry is comparable with those studied using the Euler and Navier-Stokes solvers. Further optimization scheme can readily follow.

6. Conclusion

- a. A simple geometrical configuration optimization scheme for slender axisymmetrical bodies in transonic flow for minimum drag due to afterbody contribution has been formulated and carried out, following transonic small disturbance approach and Sequential Quadratic Programming and Modified Feasible Direction optimization method. Candidate geometries can be obtained for further elaborate studies using Euler and Navier Stokes flow solvers, for inviscid and viscous cases, respectively. In addition, an analytical approach by looking into the simplified transonic gas dynamic equation following the work of Biblarz has been carried out to obtain another candidates of afterbody geometries that may be worked out further to produce the lowest drag.
- b. Further Computational Study of slender axisymmetrical body in transonic flow has also been carried out to look into the flow characteristics giving rise to the significant

- contribution to the drag from the afterbody. For practical purposes, two commercially available computational routines are utilized, these are MGAERO flow solver for the inviscid (Euler) case and the RAMPANT flow solver for the viscous (Navier-Stokes) case. Careful construction of the computational grids has been carried out to insure good accuracy.
- c. Flow characteristic of three projectile configurations, i.e one with flat base, conical and rounded afterbody, have been investigated within the transonic flow regimes. The flow characteristics exhibited the shock wave phenomena and pressure distribution along the surface that can be studied to arrive at most desirable aerodynamic characteristics. Certainly one seeks for less complex shock-wave behavior and consequently the lowest drag.
 - d. The computational study of the three geometries investigated shows that the projectile with rounded afterbody yields the lowest (optimum) drag compared to those with flat base and conical afterbody.
9. Prijono, E and Djojodihardjo, H. Computational Study Of The Aerodynamic Characteristics Of Axi-Symmetric Bodies In Transonic Flow, *Experimental and Theoretical Mechanics Conference*, Organized by Institute of Technology Bandung, (ETM 2002), 18-19 March 2002, Bali, Indonesia.
 10. Strash, D J. *MGAERO USER'S MANUAL*, Analytical Methods Inc. Redmond, Washington USA 1994.
 11. Anonymous. *RAMPANT USER'S MANUAL*. Fluent Inc, Centerra Resource Park , Lebanon, NH 03766, June 1997.

7. References and Readings

1. Ashley, H and Landahl, M.T. *Aerodynamics of Wings and Bodies.*, Addison-Wesley Publishing Co., Inc., Reading, Massachusetts, USA, 1965.
2. Krasnov, N.F. *Aerodynamics of Bodies of Revolution.* edited and annotated by D.N.Morris, Elsevier, New York.London.Amsterdam, 1970.
3. Nghiem, C.P. and Nostrud, H., Design of Axisymmetric Bodies with Minimum Transonic Drag, *AIAA Journal*, Vol.27, No.12, pp 1818-1820, 1989.
4. Biblarz, O. "An Exact Solution to the Transonic Equation", *Israel Journal of Technology*, Vol. 13, 1975.
5. Biblarz, O. and Prijono, E., Transonic Pressure Drag Coefficient for axisymmetric Bodies, *Proceeding ICAS Congress*, Anaheim, California, USA, 1994, paper no. ICAS-94-2.5.2.
6. Vanderplaats, G.N. *Numerical Optimization Techniques for Engineering Design, with Applications.* McGraw-Hill Book Company, New York, 1984.
7. Vanderplaats, G.N., Efficient Algorithm for Numerical Airfoil Optimization, *AIAA Journal of Aircraft*, vol.16, no.12, pp.842-847, December 1979.
8. Prijono, E. An Investigation of the Transonic Pressure Drag Coefficient for Axi-Symmetric Bodies, MS Thesis, Naval Postgraduate School, Monterey, CA., USA, 1994.